Comparative Genomics RNAi Screen Identifies Eftud2 as a Novel Regulator of Innate Immunity

Lesly De Arras,*,† Rebecca Laws,‡ Sonia M. Leach,† Kyle Pontis,*,† Jonathan H. Freedman,§ David A. Schwartz,†, and Scott Alper*,†**

*Integrated Department of Immunology, and †Integrated Center for Genes, Environment and Health, National Jewish Health and University of Colorado, Denver, Colorado 80206, ‡Department of Environmental Health, Boston University School of Public Health, Boston, Massachusetts 02118, §Laboratory of Toxicology and Pharmacology, National Institute of Environmental Health Sciences, National Institutes of Health, Durham, North Carolina 27709, and **Department of Medicine, University of Colorado, Aurora, Colorado 80045

ABSTRACT The extent of the innate immune response is regulated by many positively and negatively acting signaling proteins. This allows for proper activation of innate immunity to fight infection while ensuring that the response is limited to prevent unwanted complications. Thus mutations in innate immune regulators can lead to immune dysfunction or to inflammatory diseases such as arthritis or atherosclerosis. To identify novel innate immune regulators that could affect infectious or inflammatory disease, we have taken a comparative genomics RNAi screening approach in which we inhibit orthologous genes in the nematode *Caenorhabditis elegans* and murine macrophages, expecting that genes with evolutionarily conserved function also will regulate innate immunity in humans. Here we report the results of an RNAi screen of approximately half of the *C. elegans* genome, which led to the identification of many candidate genes that regulate innate immunity in *C. elegans* and mouse macrophages. One of these novel conserved regulators of innate immunity is the mRNA splicing regulator Eftud2, which we show controls the alternate splicing of the MyD88 innate immunity signaling adaptor to modulate the extent of the innate immune response.

PROPER regulation of the innate immune response is critical to prevent disease. Activation of the innate immune response can involve the recruitment and activation of phagocytic cells that produce antimicrobial compounds as well as cytokines and chemokines that recruit and stimulate other immune cells (Kaufmann 2004). A strong innate immune response also is required for a robust adaptive immune response (Lee and Iwasaki 2007; Iwasaki and Medzhitov 2010). Thus, defects in innate immune signaling can lead to enhanced susceptibility to bacterial or fungal pathogens in human patients (Picard *et al.* 2011). On the other hand chronic innate immune activation can affect a myriad of diseases with an inflammatory component including atherosclerosis, asthma, Crohn's disease, and cancer (Cook *et al.* 2004; Arcaroli *et al.* 2005; Karin and Greten

2005; Mullick *et al.* 2005; Goh and Midwood 2012). It is therefore critical that innate immunity be tightly regulated for proper human health, active when needed and inactive when not. Thus, identifying novel regulators of innate immunity could aid in the development of novel therapeutic and diagnostic options for a range of infectious and inflammatory diseases (Cook *et al.* 2004; Connolly and O'Neill 2012).

Several organisms including the nematode *Caenorhabditis elegans* have been used as models to investigate innate immunity and identify novel innate immunity regulators. While *C. elegans* lacks an adaptive immune response, it has a robust innate immune response, and has become an established model for innate immunity studies (Engelmann and Pujol 2010; Irazoqui and Ausubel 2010; Pukkila-Worley and Ausubel 2012). In response to infection, *C. elegans* produces numerous antimicrobial proteins including lysozymes, saposin-domain-containing proteins, defensin-like molecules, and many others (Ewbank 2006; Ewbank and Zugasti 2011). Production of these antimicrobials occurs in tissues exposed to pathogens and is regulated by conserved innate immune signaling pathways, including a p38 MAPK cascade,

an insulin signaling pathway, a TGFβ cascade, and others (Mochii et al. 1999; Mallo et al. 2002; Murphy et al. 2003; Couillault et al. 2004; Huffman et al. 2004; O'Rourke et al. 2006; Shapira et al. 2006; Troemel et al. 2006; Alper et al. 2007). Inhibition or mutation of genes in these conserved signaling pathways diminishes production of antimicrobial genes and enhances susceptibility to infection.

We previously used an RNAi screen to target all of the genes on C. elegans chromosome I to identify genes that regulate expression of a clec-85::gfp fusion in transgenic nematodes (Alper et al. 2008). clec-85 encodes a C-type lectin whose expression is induced by the bacterial pathogen Serratia marcescens (Mallo et al. 2002). clec-85 expression is regulated by several known innate immunity signaling pathways in C. elegans including the p38 MAPK, insulin signaling, and TGFβ signaling pathways in the presence of either pathogenic Pseudomonas aeruginosa or nonpathogenic Escherichia coli (Alper et al. 2007; Alper et al. 2008). We identified several genes on chromosome I that were required for robust clec-85 expression in the presence of the nonpathogenic bacterium E. coli. Follow-up studies using RNAi in mouse macrophages, and knockouts in C. elegans and mice validated many of these genes as novel regulators of innate immunity (Alper et al. 2008; De Arras et al. 2012, 2013). This demonstrated the utility of this comparative genomics approach for innate immune regulator gene discovery.

Here we extend this approach to C. elegans chromosomes II–IV, representing 10,862 genes and find 32 additional genes that, when inhibited by RNAi, affect expression of clec-85::gfp. In mouse macrophages, we find that 8 of 20 mammalian orthologs of these genes affect lipopolysaccharide (LPS)-induced cytokine production in mammalian cells. Overexpression studies confirm that two of these genes, Eftud2 and Atp6v1c1, regulate the response to LPS in murine macrophages. RNAi studies in C. elegans confirm that Eftud2 affects host defense in vivo. We further show that Eftud2, a component of the U5 small nuclear ribonucleoprotein (snRNP), which works with the rest of the spliceosome to regulate mRNA splicing (Kramer 1996; Fabrizio et al. 1997; Bartels et al. 2002, 2003; Brenner and Guthrie 2006; Small et al. 2006; Sperling et al. 2008; Wahl et al. 2009), regulates the innate immune response in mouse macrophages, at least in part, by controlling the alternative mRNA splicing of MyD88, a critical signaling adaptor in multiple Toll-like receptor (TLR) signaling pathways (Kawai and Akira 2010; Takeuchi and Akira 2010).

Materials and Methods

C. elegans chromosome II–IV RNAi screen to identify regulators of clec-85::gfp production

RNAi was performed in liquid culture in 96-well format as described previously (Alper et al. 2007, 2008) using the Ahringer laboratory E. coli RNAi feeding library (Kamath and Ahringer 2003; Kamath et al. 2003). In brief, dsRNA-producing bacteria were inoculated from frozen stocks into LB, grown overnight at 37°, dsRNA synthesis was induced using IPTG, the bacteria were centrifuged and resuspended in nematode growth medium, nematode eggs isolated by bleaching (Wood 1988) were added to the wells, and the nematodes were allowed to grow at 25° in the presence of the dsRNA producing bacteria for 3 days. After this incubation, each nematode was assayed using the COPAS Biosort (Union Biometrica), which assays and reports time of flight (TOF) (nematode length, a measure of nematode age) and green fluorescence (due to the clec-85::gfp fusion) in each animal. Because nematodes can sometimes get "trapped" in the Biosort and leak between wells, we performed our screen in 48 wells of each 96-well plate with a wash well between screening wells. The data were analyzed in R using slight modifications of our previously published scripts (Alper et al. 2007) (full scripts available upon request). These scripts first remove obvious outliers and noise in the data that are not due to nematodes; then the scripts generate scatterplots and boxplots, which allow us to compare nematode length and fluorescence between RNAi treatments, and report mean fluorescence and the number of worms in each well. For the genomic RNAi screen of chromosomes II–IV, scatterplots were manually screened for RNAi treatments that diminished nematode fluorescence. RNAi treatments that obviously inhibited nematode development were not considered as potential positives; these were recognized as treatments that hindered both fluorescence and nematode growth (as reflected in a decrease in time of flight). Because we presumed that any individual RNAi treatment was unlikely to have an effect, each test RNAi on the plate was compared to the other 47 RNAi treatments on that plate to look for differences.

Of the 10,862 RNAi treatments tested in the initial genomic II–IV screen, 430 genes were retested in follow-up assays. These 430 genes were reassayed by RNAi a minimum of two additional times. For the retests, bacteria and nematodes were prepared as described above, although in this case negative control dsRNA-producing bacteria (Dillin et al. 2002) were included on the assay plates. Only those genes that, when inhibited, altered clec-85::gfp fluorescence in both retests were considered positive hits. Table 1 reports the 32 positive genes with mean fluorescence compared to control. Table 1 also displays the mean fluorescence divided by the mean time of flight, which should control for variations in nematode populations. Data for the 430 genes retested, including the 32 positive hits, is presented in Supporting Information, Table S1, with the data broken down by each individual test well.

The identity of all E. coli RNAi clones that produced a phenotype was verified by DNA sequencing; clones that differed from the reported sequence are indicated in Table 1 and Table S1. We list the identity of the sequence-verified clone in these tables.

Table 1 Genes on *C. elegans* chromosomes II–IV that regulate *clec-85::gfp* expression

Clone	Worm gene	GFP (%)	GFP/TOF (%)[b]	n	Mouse ortholog	Mouse ortholog description
89H12	Y82E9BR.13	43	46	278	Als2cr12	Amyotrophic lateral sclerosis 2 (juvenile) chromosome region, candidate 12
83A3	cbp-1	48	53	155	Ep300	E1A binding protein p300
92F5	rps-24	49	63	82	Rps24	Ribosomal protein S24
121H1	vha-11	49	70	33	Atp6v1c1	ATPase, H+ transporting, lysosomal V1 subunit C1
76G3	rpn-6.1	50	63	29	Psmd11	Proteasome (prosome, macropain) 26S subunit, non-ATPase, 11
74G4	eftu-2	51	61	53	Eftud2	Elongation factor Tu GTP binding domain containing 2
31D5	T25D3.3	52	64	139	—	
81E9	far-1	53	74	149	—	
80H9	zfp-1	54	63	119	Mllt10	Myeloid/lymphoid or mixed-lineage leukemia (trithorax homolog, *Drosophila*); translocated to, 10
87B6	rpt-6	55	71	64	Psmc5	Protease (prosome, macropain) 26S subunit, ATPase 5
70D5	R74.2	55	61	137	—	
70E11	mcm-5	57	69	57	Mcm5	Minichromosome maintenance deficient 5, cell division cycle 46 (*S. cerevisiae*)
80B7	C30C11.4	58	68	74	—	
75H11	rpt-3	59	68	61	Psmc4	Proteasome (prosome, macropain) 26S subunit, ATPase, 4
69H1	rpn-1[a]	60	66	88	Psmd2	Proteasome (prosome, macropain) 26S subunit, non-ATPase, 2
107B12	rpn-7	63	80	101	Psmd6	Proteasome (prosome, macropain) 26S subunit, non-ATPase, 6
92G7	W03G1.5	63	74	61	Catsper1	Cation channel, sperm associated 1
92C9	dpy-9	64	72	190	—	
51E1	hel-1	65	69	126	Ddx39a	DEAD (Asp-Glu-Ala-Asp) box polypeptide 39
71H8	F26A1.3	67	72	374	Ttbk1	Tau tubulin kinase 1
67G1	fbxa-30	68	70	185	—	
84H7	W09D10.1	69	78	151	Smap1	Stromal membrane-associated protein 1
31D11	T01D1.5	69	74	253	—	
76D7	lim-8	71	74	92	Lmo7	LIM domain only 7
31D7	T01D1.1	72	80	182	—	
107F12	spp-18[a]	74	82	334	—	
86D2	C24H11.1	76	88	71	Ppp1cb	Protein phosphatase 1, catalytic subunit, beta isoform
84B9	T07A5.7[a]	76	88	108	—	Fukutin
82D4	clu-1	78	86	169	1300001I01Rik	—
107C12	T20D3.6	80	82	325	Higd1b	HIG1 domain family, member 1B
56B4	C07E3.3	81	84	214	—	
116C12	tag-273[a]	84	84	379	—	

[a] Sequencing of the RNAi clone identified a different gene than the predicted gene; the correct (sequenced) gene is listed here.
[b] GFP/TOF is the mean GFP level normalized to nematode size.

Use of RNAi in mouse macrophages to test candidate genes

Orthologs of *C. elegans* genes were identified using either the Homologene database at the National Center for Biotechnology Information or the Panther database from within WormBase (Mi *et al.* 2010; Sayers *et al.* 2012; Yook *et al.* 2012). RNAi was performed largely as described previously (Alper *et al.* 2008). Briefly, either pools of siRNA duplexes or individual siRNA duplexes (Dharmacon) were transfected into the mouse macrophage cell line RAW264.7 using the Amaxa 96-well nucleofector shuttle. Cells were then plated at either 100,000 cells/well in 96-well format (for ELISAs) or 200,000 cells/well in 24-well format (for qPCR). Negative control siRNAs included Dharmacon's nontargeting siRNA pool no. 1 and nontargeting siRNA no. 1. Twenty-four hours after transfection, cells were incubated in the presence of 20 ng/ml LPS (List Biological Labs), and supernatants were collected for ELISA (R&D Systems). In the primary screen, we monitored the production of IL-6 as we have found this to be a more responsive readout than TNFα or other cytokines in response to most RNAi treatments (Alper *et al.* 2008; De Arras *et al.* 2013). The cells were then either subjected to viability analysis using fluorescien diacetate as described (Fernandez‑Botran and Větvička 2001) or lysed in RLT buffer (Qiagen) for RNA preparation for qPCR and RT–PCR. RNA was purified using the RNeasy kit (Qiagen), and qPCR was performed using the Quantitect SYBR Green RT–PCR kit (Qiagen) on an ABI 7900 thermocycler. Conditions for qPCR and RT-PCR to monitor MyD88$_L$ and MyD88$_S$ were as described previously (De Arras and Alper 2013). Expression levels were normalized using β-actin as a control; all primer sequences are listed in Table S2.

In one set of experiments, both Eftud2- and MyD88$_S$-specific siRNA were delivered simultaneously. In the controls for this experiment when only a single siRNA was used, an equivalent volume of nontargeting control siRNA was included as well.

Overexpression studies in mouse macrophages

Plasmids containing full-length cDNAs cloned downstream of the CMV promoter were obtained for Eftud2 (Origene); Rps24, Atp6v1c1, and Mcm5 (Open Biosystems); and negative control chloramphenicol acetyltransferase (CAT, Invitrogen). Transient transfections were performed using 3.75 µl Fugene HD (Roche) with 100,000 cells in 24-well format and contained 300 ng IL-6-luciferase, 100 ng SV40-rluc (Promega), and 600 ng of overexpression plasmid. Twenty-four hours after transfection, cells were stimulated with LPS for 6 hr and then luciferase activity was monitored using the Dual luciferase assay kit (Promega) using SV40-rluc as a normalization control for transfection efficiency. Stable Eftud2-overexpressing lines were generated by transfecting the CMV-Eftud2 plasmid (200 ng into 200,000 cells, 12-well format) and selecting with G418.

C. elegans survival assays

Survival assays in the presence of either *P. aeruginosa* strain PA14 (Rahme *et al.* 1995; Mahajan-Miklos *et al.* 1999; Tan *et al.* 1999) or *E. coli* strain OP50 (Wood 1988) were performed largely as described previously (Alper *et al.* 2010) with the following modifications. The RNAi hypersensitive strain GR1373 *eri-1(mg366) IV* (Kennedy *et al.* 2004) was synchronized by collecting hatchlings at 15° (Wood 1988), the hatchlings were moved to *E. coli*-expressing dsRNA and incubated at 25° for 24 hr until they were in the late L4 stage, and then the nematodes were exposed to either PA14 or OP50 at 25° in the presence of 5 µg/ml of the sterilizing agent 5-fluoro-2-deoxyuridine (Mitchell *et al.* 1979) on modified NGM plates (Powell and Ausubel 2008). In the heat-killed bacteria experiment, a liquid OP50 culture was concentrated fivefold, incubated at 80° for 3 hr, and plated on modified NGM supplemented with kanamycin. Inhibition of *eftu-2* or *vha-11* in the *eri-1* mutant background caused the nematodes to develop smaller and thinner than control-treated animals.

Statistical analyses

The analyses of the nematode RNAi data are described above. *C. elegans* survival assays were performed in triplicate and were analyzed using GraphPad Prism 5. All macrophage experiments were performed with a minimum of three independent biological replicates, and in the case of the follow-up assays, were performed numerous additional times. Statistical analyses were performed using unpaired *t*-tests in GraphPad Prism 5; significance was considered $P < 0.05$.

Results

Genomic RNAi screen of C. elegans chromosomes II–IV

We used an *E. coli* library that expresses dsRNA corresponding to most genes in the *C. elegans* genome (Kamath and Ahringer 2003; Kamath *et al.* 2003) to systematically inhibit each gene on chromosomes II–IV, and then monitored the effect on fluorescence in *clec-85::gfp* transgenic nematodes
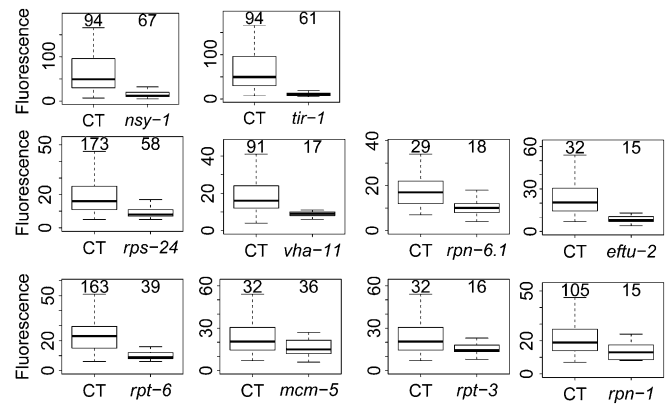
Figure 1 Identification of genes on *C. elegans* chromosomes II–IV that regulate *clec-85::gfp* expression. *clec-85::gfp* transgenic nematodes were subjected to either the indicated test RNAi treatment or control (CT) RNAi treatment and fluorescence in these nematodes was assayed using the COPAS Biosort, which reports GFP-mediated fluorescence and time of flight (TOF, which measures nematode length, a measure of nematode age) for each animal. The boxplots display fluorescence data for TOF ranging from 150 to 350 with the black bar representing the median and the box extending from the 25th to the 75th percentiles. Individual *n* values are displayed above each boxplot.

using the COPAS Biosort (essentially a nematode flow cytometer). As a control, we found that *clec-85::gfp* expression is strongly diminished when either *nsy-1* or *tir-1* are inhibited (Figure 1, top). *nsy-1* is the MAPKKK that acts upstream of the p38 MAP kinase in *C. elegans*; *tir-1* is the sole *C. elegans* MyD88 family member. Both *nsy-1* and *tir-1* are required for expression of numerous antimicrobial genes and resistance to Gram negative and positive bacteria and fungi (Kim *et al.* 2002; Couillault *et al.* 2004; Liberati *et al.* 2004; Alper *et al.* 2007; Bolz *et al.* 2010; Muhammed *et al.* 2012).

We screened through ∼10,862 genes by RNAi and monitored fluorescence in these nematodes. Of these 10,862 genes tested, we identified 430 genes whose inhibition led to diminished *clec-85::gfp* fluorescence without significantly diminishing overall nematode size. RNAi treatments that affect development or overall fitness are predicted to diminish both fluorescence as well as nematode size (a marker of growth and development) and were not considered further. We retested these 430 gene candidates, performing the assays a minimum of two more times. Of these 430 retested candidates, RNAi-mediated inhibition of 32 genes led to decreased *clec-85::gfp* fluorescence in both retests as well as in the original genomic screen [list of 32 hits in Table 1, boxplots for genes that also affect macrophage immunity (see below) in Figure 1 rows 2 and 3, compilation of all retest data in Table S1]. Thus, we identified 32 genes on *C. elegans* chromosomes II–IV that affected production of the candidate antimicrobial gene *clec-85* and that are therefore potentially novel innate immune regulators. Many of these candidates function in various catabolic pathways (Table S3, analysis performed using the Gather Utility) (Chang and Nevins 2006), suggesting that catabolism could modulate innate immunity in *C. elegans*.

RNAi in mouse macrophages to monitor innate immune regulatory function of novel candidate genes

Twenty of these 32 novel candidates identified in *C. elegans* have an ortholog in mice (Table 1). To examine the potential innate immune regulatory function of these mammalian genes, we inhibited these 20 genes using RNAi in the mouse macrophage cell line RAW264.7, stimulated the cells with LPS, and monitored production of the proinflammatory cytokine IL-6. As a positive control, we found that treatment of these cells with siRNA that targeted TLR4, the LPS receptor, strongly inhibited LPS-induced IL-6 production (Figure 2A). Inhibition of 7 of our 20 novel candidates using pools of siRNA duplexes targeting each gene led to a statistically significant decrease in IL-6 production (Figure 2A); in contrast, inhibition of several other genes significantly increased IL-6 production (Figure 2A). As a control, we found that these siRNA treatments, with the exception of Rps24 siRNA, did not significantly diminish cell viability (Figure 2B).

We took several steps to confirm these RNAi data and to confirm that the effects were due to specific inhibition of the corresponding endogenous gene and not an off-target siRNA effect. We focused on the seven genes whose inhibition led to decreased IL-6 production and the two genes whose inhibition had the strongest effect on increased IL-6 production. First, we used qPCR to demonstrate that the siRNA treatments were inhibiting production of the corresponding endogenous gene; we found that gene-specific knockdown was statistically significant for eight of these nine siRNAs, but could not validate knockdown for one gene, Ttbk1 (Figure 2C). To further verify that the effects were due to inhibition of the corresponding endogenous gene, we also demonstrated that at least two individual siRNA duplexes targeting each gene induced a similar phenotype. We were able to validate the data for eight of the nine gene targets, with the exception of Ttbk1, where none of the individual siRNA duplexes diminished LPS-induced IL-6 production (Figure S1). Multiple siRNA duplexes targeting the same gene induced the same phenotype, which suggested that the altered LPS-induced cytokine production was due to inhibition of that gene. Thus, we conclude that with the exception of Ttbk1, eight of these nine novel candidate genes do regulate the extent of LPS-induced IL-6 production. Four of the genes that affected the LPS response were components of the 26S proteasome (Psmd2, Psmc5, Psmd11, Psmc4); however, siRNA-mediated inhibition of another 26S proteasome subunit (Psmd6) did not affect the LPS response (Figure 2A), despite relatively strong Psmd6 knockdown as assayed with either of two sets of qPCR primers (Figure S2).

Overexpression studies in mouse macrophages to monitor innate immune regulatory function of novel candidate genes

Our RNAi studies identified eight potential candidate innate immunity regulators, including six genes whose inhibition diminished LPS-induced IL-6 production (four proteasome subunits Psmd2, Psmc5, Psmd11, and Psmc4; the ribosomal
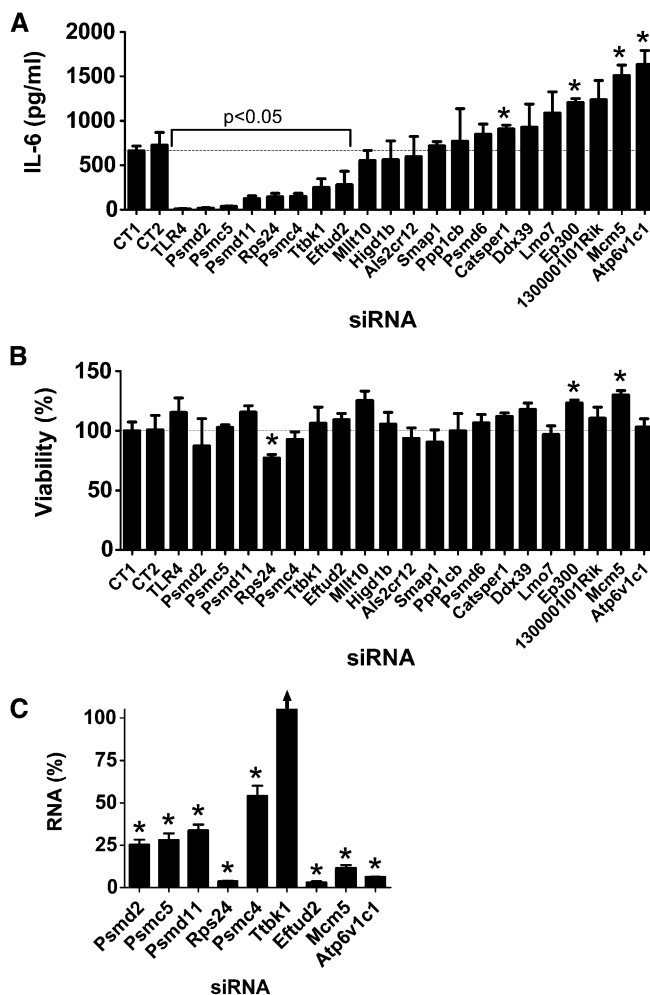
Figure 2 Use of siRNA pools to identify genes that regulate LPS-induced IL-6 production in murine macrophages. Pools of siRNA duplexes targeting the indicated genes (or nontargeting control pools CT1 or CT2) were transfected into the mouse macrophage cell line RAW264.7; the cells were stimulated for 6 hr with 20 ng/ml LPS; and IL-6 protein production (A), cell viability (B), or siRNA-mediated gene knockdown (C) was monitored. All plots display mean ± SEM. Asterisks in this figure and subsequent figures indicate values that were significantly different from control ($P < 0.05$). The arrow for Ttbk1 in C indicates an RNA value that is off scale (156%).

protein Rps24; and the mRNA splicing regulator Eftud2) and two genes whose inhibition enhanced LPS-induced IL-6 production (Mcm5 and Atp6v1c1). To further investigate the potential innate immune regulatory function of these genes, we chose to overexpress some of them and monitor the effect on IL-6 transcription using an IL-6-luciferase reporter construct (Baccam *et al.* 2003). If overexpression induced a phenotype opposite to that caused by RNAi, that would confirm the importance of that gene in innate immunity regulation. In contrast, lack of a phenotype is not necessarily informative.

The 26S proteasome is known to regulate the LPS response (Shen *et al.* 2006), so we chose to focus on the other four potentially novel candidates. We transiently
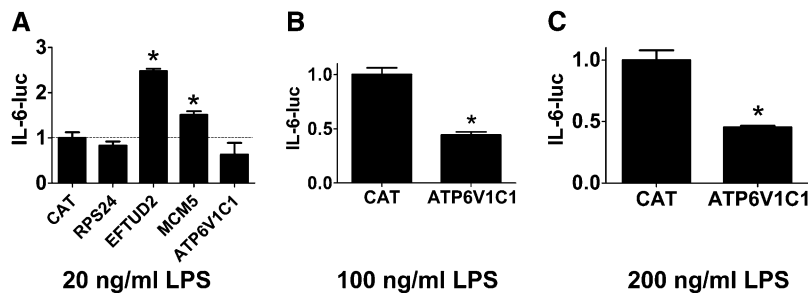
Figure 3 Overexpression studies demonstrate that Eftud2 and Atp6v1c1 regulate IL-6 expression. Plasmids overexpressing the indicated genes were cotransfected along with plasmids expressing IL-6-luciferase and SV40-rluc into RAW264.7 cells, the cells were stimulated with the indicated quantities of LPS for 6 hr, and IL-6-luc activity (normalized to SV40-rluc) was monitored.

transfected IL-6-luciferase, SV40-rluc for normalization, and plasmids that overexpress each of Rps24, Eftud2, Mcm5, and Atp6v1c1 using the strong CMV promoter into the mouse macrophage cell line RAW264.7 and monitored IL-6-luc production in the presence of 20 ng/ml LPS. As a negative control, we also transfected a plasmid that overexpressed CAT, which should not affect innate immunity. Rps24 overexpression did not have a significant effect on IL-6-luc production (Figure 3A), and Mcm5 overexpression induced a moderate increase in IL-6-luc production (Figure 3A), which is similar to the effect observed with RNAi, so we cannot draw any further conclusions about the role of Rps24 or Mcm5 in innate immunity based on these overexpression data. In contrast, overexpression of Eftud2 strongly enhanced IL-6-luc production (Figure 3A), a phenotype opposite to that of Eftud2 siRNA. Similarly, Atp6v1c1 overexpression decreased IL-6-luc expression, a phenotype that also is opposite to the RNAi-induced phenotype, although this decrease was not statistically significant (Figure 3A). To explore the function of Atp6v1c1 further, we overexpressed Atp6v1c1 in the presence of higher doses of LPS and found that Atp6v1c1 did significantly inhibit IL-6-luc expression under those conditions (Figure 3, B and C). Thus, the RNAi and overexpression data indicate that wild-type Eftud2 enhances LPS-induced IL-6 expression while wild-type Atp6v1c1 diminishes LPS-induced IL-6 expression.

eftu-2/Eftud2 regulates host defense in C. elegans

To test the potential innate immune regulatory function of Eftud2 and Atp6v1c1 *in vivo*, we inhibited these two genes by RNAi in *C. elegans*, exposed these nematodes to the nematode and human pathogen *P. aeruginosa* strain PA14, and then monitored survival of the animals. We inhibited either *eftu-2* or *vha-11* (the *C. elegans* orthologs of Eftud2 and Atp6v1c1, respectively) in nematodes harboring a mutation in *eri-1*, which enhances nematode RNAi sensitivity. Inhibition of either gene diminished survival of nematodes exposed to *P. aeruginosa* compared to animals exposed to control RNAi bacteria (Figure 4A). However, inhibition of *vha-11* also diminished survival in the presence of the nonpathogenic *E. coli* strain (Figure 4B). Because live *E. coli* can be slightly pathogenic to *C. elegans* (Garsin *et al.* 2001; Tenor and Aballay 2007), we also monitored survival of *vha-11(RNAi)* animals in the presence of heat-killed *E. coli*. Under these conditions, inhibition of *vha-11* still diminished

nematode survival (Figure 4C). Thus, we cannot differentiate the effects of *vha-11* in *C. elegans* between an effect on fitness or an effect on both fitness and host defense. In contrast, nematodes exposed to *eftu-2* RNAi lived as long as or slightly longer than control RNAi-treated nematodes in the presence of nonpathogenic *E. coli* (Figure 4B). Thus, *eftu-2*/Eftud2 is specifically affecting host defense and not fitness in *C. elegans*.

Eftud2 is a novel innate immunity regulator in mouse macrophages

Based on the siRNA and overexpression data in macrophages and the *in vivo* survival data in *C. elegans*, we chose to investigate the function of Eftud2 further. First, we performed additional siRNA experiments in macrophages using a slightly higher dose of Eftud2 siRNA to see if this could enhance the phenotype; we found that this led to a greater inhibition in LPS-induced IL-6 protein production (Figure 5A). Inhibition of Eftud2 also diminished IL-6 mRNA production (Figure 5B). The effect of Eftud2 was not limited to IL-6 as production of the proinflammatory cytokine TNFα also was diminished when Eftud2 was inhibited by siRNA (Figure 5C). As further confirmation that transient Eftud2 overexpression enhanced IL-6-luciferase expression, we overexpressed Eftud2 in the presence of a second higher LPS dose of 50 ng/ml (Figure 5D) and found that Eftud2 enhanced IL-6 transcription at this higher LPS dose as well. To further test the function of Eftud2, we generated stable RAW264.7 lines overexpressing Eftud2, and as expected, found that stable Eftud2 overexpression enhanced LPS-induced production of IL-6 and TNFα (Figure 5, E and F). All these data indicate that wild-type Eftud2 enhances LPS-induced IL-6 production by enhancing IL-6 expression.

Eftud2 regulates alternative splicing of MyD88 to control the innate immune response in macrophages

Eftud2 is a component of the U5 snRNP, which functions with the rest of the spliceosome to control mRNA splicing (Kramer 1996; Fabrizio *et al.* 1997; Bartels *et al.* 2002, 2003; Brenner and Guthrie 2006; Small *et al.* 2006; Sperling *et al.* 2008; Wahl *et al.* 2009). We previously found that SF3a and SF3b, which function with the U2 snRNP to control mRNA splicing (Kramer *et al.* 2005; Sperling *et al.* 2008; Collins *et al.* 2009; Rino and Carmo-Fonseca 2009; Wahl *et al.* 2009), also regulate the extent of the innate immune
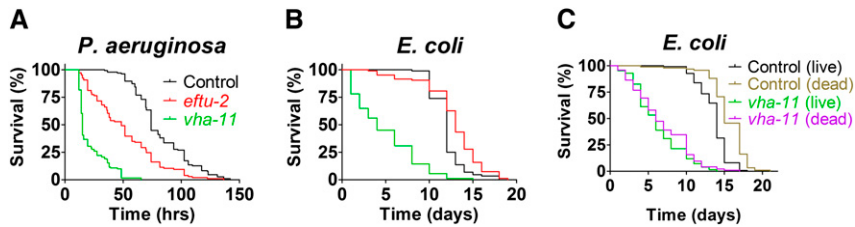
Figure 4 *eftu-2*/Eftud2 regulates host defense in *C. elegans*. Depicted are survival plots for *eri-1* mutant nematodes treated with either control RNAi, *eftu-2* RNAi, or *vha-11* RNAi (as indicated) that were subsequently exposed to either *P. aeruginosa* strain PA14 (A), live *E. coli* strain OP50 (B and C), or heat-killed OP50 (C). Further statistical data (medians, *n*, and *P*-values) are presented in Table S4.

response (De Arras and Alper 2013). SF3a and SF3b affect innate immunity in mouse macrophages, at least in part, by regulating alternative splicing of MyD88 (De Arras and Alper 2013). MyD88 is a signaling adaptor that functions downstream of most TLRs (Kawai and Akira 2010; Takeuchi and Akira 2010). Full-length MyD88 is encoded by a five-exon mRNA (long form or MyD88$_L$). However, a shorter MyD88 mRNA (MyD88$_S$) that lacks exon 2 encodes a negative regulator of TLR signaling (Janssens *et al.* 2002; Burns *et al.* 2003; Janssens *et al.* 2003; Adib-Conquy *et al.* 2006; Mendoza-Barbera *et al.* 2009). Inhibition of SF3a or SF3b using siRNA or a pharmacological agent diminishes LPS-induced IL-6 and TNFα production, at least in part, by enhancing production of the negatively acting MyD88$_S$ splice form (De Arras and Alper 2013). We therefore chose to monitor if the Eftud2 mRNA splicing regulator likewise affects alternative splicing of MyD88.

To monitor MyD88$_L$ and MyD88$_S$ levels when Eftud2 was inhibited, we used a qPCR assay and primer sets that can distinguish between the two mRNA splice forms (De Arras and Alper 2013). We inhibited Eftud2 using siRNA, stimulated the cells with 20 ng/ml LPS for 6 hr, and then monitored the two MyD88 mRNA splice forms by qPCR. Eftud2 inhibition led to a moderate decrease in MyD88$_L$ levels and a substantial increase in MyD88$_S$ levels (Figure 6, A and B). In contrast, Eftud2 inhibition did not affect all mRNA splicing events as intron 3 of actin was excised normally (data not shown).

We also used semiquantitative RT–PCR and subsequent agarose gel electrophoresis to monitor the two MyD88 mRNA splice forms. RT–PCR using primers specific to the MyD88$_S$ mRNA splice form demonstrated that inhibition of Eftud2 by RNAi led to increased MyD88$_S$ production (Figure S3, A and B), confirming the qPCR data. In contrast, production of β-actin was not significantly affected (Figure S3, A and C). Using primers that bracketed exon 2, we also were able to amplify products corresponding to both MyD88$_L$ and MyD88$_S$ simultaneously. As observed previously (De Arras and Alper 2013), there is substantially more MyD88$_L$ than MyD88$_S$ in unstimulated cells (Figure 6G). Inhibition of Eftud2 by RNAi led to a significant decrease in MyD88$_L$ and a concomitant increase in the smaller MyD88$_S$ form (Figure 6G and Figure S3, D and E).

The increased amount of the MyD88$_S$ inhibitory splice form could explain in whole or in part the weakened LPS response when Eftud2 is inhibited. To directly test if Eftud2's effect on innate immunity is mediated by changes

in MyD88$_S$ levels, we chose to inhibit the MyD88$_S$ mRNA splice form when Eftud2 was inhibited in an attempt to restore LPS-induced IL-6 production. To decrease MyD88$_S$ mRNA levels, we used a siRNA that targets the unique exon 1–exon 3 splice junction that is present in MyD88$_S$ but absent in MyD88$_L$ (De Arras and Alper 2013). Treatment of cells with this MyD88$_S$ siRNA leads to a moderate increase in LPS-induced IL-6 production (Figure 6C; in other experiments not shown, this increase was more significant). We found that treatment of cells with Eftud2 siRNA alone strongly diminished LPS-induced IL-6 production while treatment of cells with both Eftud2 siRNA and MyD88$_S$ siRNA simultaneously strongly rescued LPS-induced IL-6 production Figure 6C). As a control, we verified that the siRNAs were inducing similar knockdown under the various conditions (Figure 6, D–F). This suggests that much of the effect of Eftud2 on the LPS response is mediated by altered MyD88 mRNA splicing.

Discussion

Identification of novel conserved regulators of innate immunity using comparative genomics

Our hypothesis is that genes with evolutionarily conserved innate immune regulatory function in *C. elegans* and murine macrophages will likely also affect humans and are therefore candidate regulators of human infectious and inflammatory disease. Our comparative genomics RNAi screening approach in *C. elegans* and mouse macrophages has identified many such candidate innate immune regulators (this study and Alper *et al.* 2008; De Arras *et al.* 2013). One advantage of this approach is that it may overcome the high false-positive rate present in mammalian RNAi screens due to off-target effects (Editorial 2003). Thus far, we have validated many of these dual RNAi hits (nematodes and macrophages) using knockout mutations in *C. elegans* and have validated two dual RNAi hits using mouse knockouts (Alper *et al.* 2008; De Arras *et al.* 2012, 2013).

The *C. elegans* screening approach is an efficient one for identifying innate immunity regulators, as we see a 30–40% hit rate translating genes from nematodes to macrophages (Alper *et al.* 2008; De Arras *et al.* 2013; and the current study, which is far higher than other approaches that we have taken (for example, we had a 2% hit rate monitoring a set of 100 genes identified as candidate innate immunity regulators based on a computational analysis of their expression
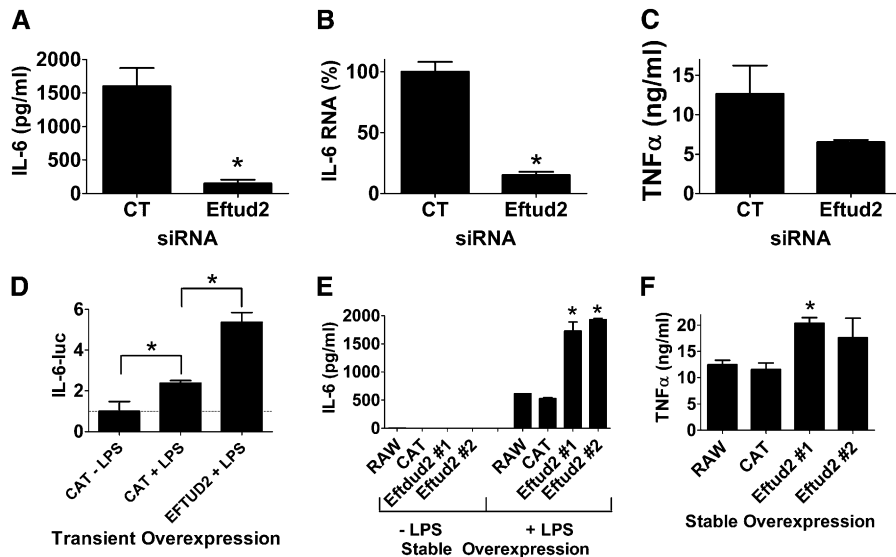
Figure 5 Eftud2 regulates the innate immune response in mouse macrophages. (A–C) Cells were treated with either Eftud2 siRNA or control (CT) siRNA; were exposed to 20 ng/ml LPS for 6 hr; and IL-6 protein (A), IL-6 mRNA (B), or TNFα protein (C) was monitored. (D) Cells were transiently transfected with plasmids expressing IL-6-luciferase, SV40-rluc, and either Eftud2 or CAT; were exposed to 50 ng/ml LPS for 6 hr where indicated; and IL-6-luc production (normalized relative to SV40-rluc) was monitored. (E and F) Cell lines stably overexpressing Eftud2, CAT, or the parent RAW264.7 cell line were stimulated with 20 ng/ml LPS for 6 hr and cytokine production was monitored.

levels in the Gene Expression Omnibus database, data not shown). One unanswered question is: Are these genes regulating innate immunity in a similar fashion in both species? This is particularly relevant as many of the candidates identified in the current study are components of the 26S proteasome, which regulates innate immunity in *Drosophila* and mammals by degrading IκB, thereby allowing NFκB activation (Coux *et al.* 1996; Foley and O'Farrell 2004). However, while *C. elegans* has an IκB homolog, as yet no direct NFκB homolog has been identified (Pujol *et al.* 2001). It could be that another gene serves a similar function in *C. elegans*, or it could be that the 26S proteasome regulates innate immunity in *C. elegans* by a different mechanism. Nevertheless, this comparative genomics approach seems to be an efficient way to find novel genes that matter.

There is precedent in *C. elegans* for innate immunity genes in *C. elegans* acting in both conserved and novel fashion. The p38 MAPK pathway acts similarly in both *C. elegans* and mammals (Kim *et al.* 2002). In contrast, while the Xbp1 transcription factor enhances host defense in both mammals and *C. elegans*, it does so by different mechanisms: by acting as a TLR-signaling dependent transcriptional activator that functions with NFκB in mice (Martinon *et al.* 2010) and by playing a detoxification role in the immune response in *C. elegans* (Richardson *et al.* 2010). Thus, while we see a high degree of "conservation of function" of innate immunity regulators, it is as yet unclear if there is "conservation of mechanism," although given the reported differences in *C. elegans* innate immunity, we speculate that many of these genes may use different mechanisms in the different species to effect host defense.

Many of our candidate genes encoded components of the 26S proteasome, which is already the target of potential therapeutic pharmacological options (Elliott *et al.* 2003; Wang and Maldonado 2006; Calzado *et al.* 2007). We note that while siRNA-mediated inhibition of several 26S proteasome subunits strongly diminished LPS-induced cytokine production, the inhibition of Psmd6 did not. This raises the possibility of either differential function or differential sensitivity of different 26S proteasome subunits to inhibition, suggesting that targeting individual subunits of the 26S proteasome using siRNA could be another approach to treat inflammatory diseases.

The role of Atp6v1c1 in innate immunity regulation

Our RNAi and overexpression data indicate that Atp6v1c1 limits the innate immune response by diminishing IL-6 transcription. Atp6v1c1 is the VMA5 subunit of the vacuolar H$^+$-ATPase (V-ATPase) (Smith *et al.* 2003). The V-ATPase is a large multiprotein complex that mediates acidification of intracellular organelles and can therefore affect numerous biological processes (Stevens and Forgac 1997; Forgac 1999; Nishi and Forgac 2002). Atp6v1c1 helps mediate the assembly of the catalytic and membrane portions of the V-ATPase (Ho *et al.* 1993; Drory *et al.* 2004). Inhibition of the V-ATPase in macrophages using the pharmacological agent bafilomycin A1 enhances LPS-induced NFκB activation and cytokine production (Bidani and Heming 1995; Conboy *et al.* 1999), which is consistent with our RNAi and overexpression data. This suggests that activating individual V-ATPase subunits could also be a potential therapeutic option for inflammatory diseases.

The Eftud2 mRNA splicing regulator controls innate immunity by altering MyD88 mRNA splicing

Another novel innate immunity regulator identified by our comparative genomics approach is Eftud2, a component of the U5 snRNP in the spliceosome that mediates pre-mRNA splicing (Kramer 1996; Fabrizio *et al.* 1997; Bartels *et al.* 2002, 2003; Brenner and Guthrie 2006; Small *et al.* 2006; Sperling *et al.* 2008; Wahl *et al.* 2009). Consistent with its role as a general mRNA splicing regulator, *C. elegans* eftu-2/Eftud2 has been implicated in a variety of developmental processes, including the organization of myofilaments and
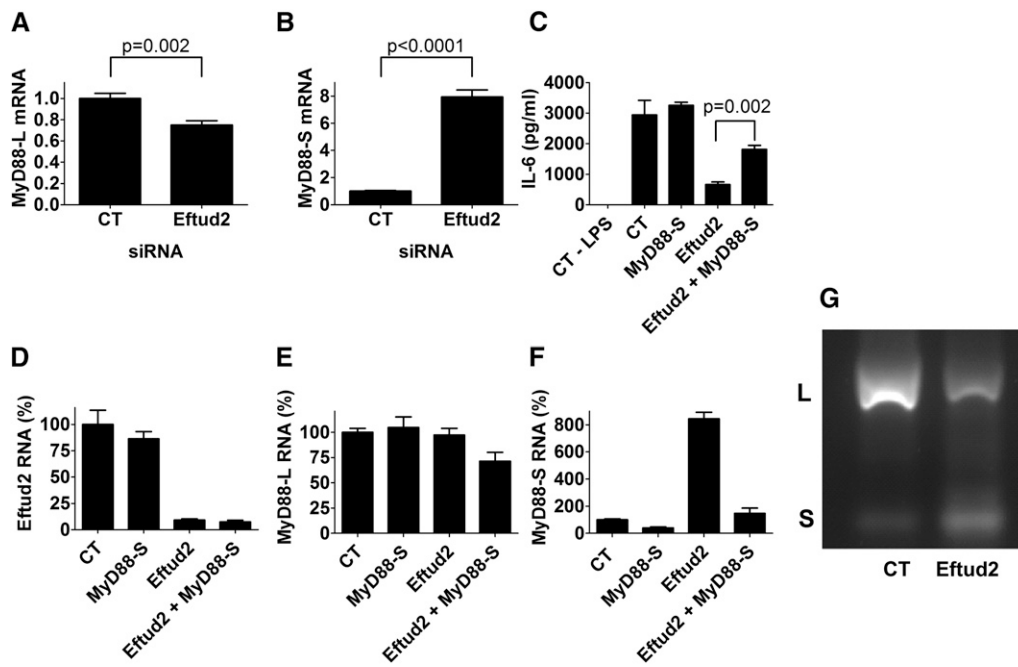
Figure 6 Eftud2 regulates innate immunity by controlling the alternative mRNA splicing of MyD88. (A and B) Cells were treated with either Eftud2 siRNA or control (CT) nontargeting siRNA, were stimulated with 20 ng/ml LPS for 6 hr, and $MyD88_L$ and $MyD88_S$ mRNA levels were monitored by qPCR. (C–F) Cells were treated with the indicated siRNAs, were stimulated with 20 ng/ml LPS for 6 hr, and either IL-6 was monitored by ELISA (C) or Eftud2, $MyD88_L$, and $MyD88_S$ mRNA levels were monitored by qPCR (D–F). mRNA levels were normalized such that 100% indicates mRNA in the presence of control RNAi in the absence of LPS. (G) Cells were exposed to either Eftud2 siRNA or control nontargeting siRNA (CT), were then treated with 20 ng/ml LPS for 6 hr, RNA was extracted, RT–PCR was performed to amplify the indicated mRNAs, and the amplified products were analyzed by agarose gel electrophoresis. Representative image is shown of PCR products using primers that bracket MyD88 exon 2 and that therefore simultaneously generate a 280-bp product corresponding to $MyD88_L$ and a 145-bp product corresponding to $MyD88_S$.

P granule development (Meissner *et al.* 2009; Updike and Strome 2009). In humans, mutations in Eftud2 cause craniofacial conditions including mandibulofacial dysostosis and esophageal atresia (Gordon *et al.* 2012; Lines *et al.* 2012; Luquetti *et al.* 2013; Voigt *et al.* 2013).

In the present study, we found that inhibition of Eftud2 diminished LPS-induced IL-6 and TNFα production while overexpression of Eftud2 enhanced cytokine production. At least part of this effect occurs at the IL-6 transcriptional level. Importantly, inhibition of Eftud2 did not affect overall cell viability, suggesting that at this level of gene inhibition, the innate immune response is far more sensitive to Eftud2 levels than are other general cell functions.

These data are reminiscent of the effects of the SF3a and SF3b complexes that interact with the U2 snRNP to facilitate mRNA splicing (Kramer *et al.* 2005; Sperling *et al.* 2008; Collins *et al.* 2009; Rino and Carmo-Fonseca 2009; Wahl *et al.* 2009). We previously reported that inhibition of SF3a or SF3b by RNAi or a pharmacological agent diminished LPS-induced cytokine production in mouse macrophages (De Arras and Alper 2013). SF3a and SF3b regulate innate immunity in part by modulating alternative splicing of MyD88 (De Arras and Alper 2013). The five exon full-length long form $MyD88_L$ encodes a critical signaling adaptor in multiple TLR response pathways. In contrast, the shorter splice form $MyD88_S$ that lacks the 135-bp exon 2 encodes an in-frame protein that is a negative regulator of TLR signaling, which prevents activation of the downstream signaling IRAK proteins (Janssens *et al.* 2002; Burns *et al.* 2003; Mendoza-Barbera *et al.* 2009). Because of the similarity in the effects of

SF3a/b and Eftud2 inhibition, we monitored MyD88 mRNA splicing when Eftud2 was inhibited and found that the inhibitory splice form $MyD88_S$ was increased dramatically, which is consistent with the resulting diminished cytokine response. Moreover, we were able to partially rescue the defect caused by Eftud2 inhibition by normalizing $MyD88_S$ levels with a second $MyD88_S$-specific siRNA. Thus, SF3a, SF3b, and Eftud2 all are required for retention of exon 2 in MyD88, as this exon is lost and $MyD88_S$ is produced when any of these spliceosome components are inhibited. This result is consistent with other reports that show that inhibition of specific spliceosome subunits leads to alternative splicing and exon skipping (Corrionero *et al.* 2011; Fan *et al.* 2011; An and Henion 2012; Visconte *et al.* 2012). Moreover, the current data show that regulators of the U2 snRNP (SF3a and SF3b), which affect 3′ splice site choice, and the U5 snRNP (Eftud2), which joins the spliceosome at a later stage of assembly (Newman 1997; Turner *et al.* 2004; Wahl *et al.* 2009), both have similar effects on MyD88 mRNA splicing.

The *C. elegans* and mouse orthologs of Eftud2, SF3a1, and SF3b1 exhibit 70, 45, and 67% identity, respectively. While Eftud2 regulates innate immunity in both species, it is unclear how much mechanistic conservation there is. While the sole *C. elegans* MyD88 family member *tir-1* also exhibits alternate splicing, no alternate functions have been reported for these splice forms in innate immunity, and the relevant intron–exon junctions in MyD88 do not appear to be conserved in *tir-1* (data not shown).

$MyD88_S$ levels are increased ∼10-fold in monocytes from septic patients (Adib-Conquy *et al.* 2006), suggesting that

a better understanding of the regulation of MyD88 mRNA splicing could contribute to our understanding and ability to treat inflammatory disease. The identification of Eftud2 as a novel regulator of MyD88 mRNA splicing and innate immunity should further this approach.

Acknowledgments

Literature Cited

Adib-Conquy, M., C. Adrie, C. Fitting, O. Gattolliat, R. Beyaert et al., 2006   Up-regulation of MyD88s and SIGIRR, molecules inhibiting Toll-like receptor signaling, in monocytes from septic patients. Crit. Care Med. 34: 2377–2385.

Alper, S., S. J. McBride, B. Lackford, J. H. Freedman, and D. A. Schwartz, 2007   Specificity and complexity of the C. elegans innate immune response. Mol. Cell. Biol. 27: 5544–5553.

Alper, S., R. Laws, B. Lackford, W. A. Boyd, P. Dunlap et al., 2008   Identification of innate immunity genes and pathways using a comparative genomics approach. Proc. Natl. Acad. Sci. USA 105: 7016–7021.

Alper, S., M. McElwee, J. Apfeld, B. Lackford, J. Freedman et al., 2010   Germline proliferation regulates distinct signaling pathways in C. elegans to control lifespan and innate immunity. J. Biol. Chem. 285: 1822–1828.

An, M., and P. D. Henion, 2012   The zebrafish sf3b1b460 mutant reveals differential requirements for the sf3b1 pre-mRNA processing gene during neural crest development. Int. J. Dev. Biol. 56: 223–237.

Arcaroli, J., M. B. Fessler, and E. Abraham, 2005   Genetic polymorphisms and sepsis. Shock 24: 300–312.

Baccam, M., S. Y. Woo, C. Vinson, and G. A. Bishop, 2003   CD40-mediated transcriptional regulation of the IL-6 gene in B lymphocytes: involvement of NF-kappa B, AP-1, and C/EBP. J. Immunol. 170: 3099–3108.

Bartels, C., C. Klatt, R. Luhrmann, and P. Fabrizio, 2002   The ribosomal translocase homologue Snu114p is involved in unwinding U4/U6 RNA during activation of the spliceosome. EMBO Rep. 3: 875–880.

Bartels, C., H. Urlaub, R. Luhrmann, and P. Fabrizio, 2003   Mutagenesis suggests several roles of Snu114p in pre-mRNA splicing. J. Biol. Chem. 278: 28324–28334.

Bidani, A., and T. A. Heming, 1995   Effects of bafilomycin A1 on functional capabilities of LPS-activated alveolar macrophages. J. Leukoc. Biol. 57: 275–281.

Bolz, D. D., J. L. Tenor, and A. Aballay, 2010   A conserved PMK-1/p38 MAPK is required in C. elegans tissue-specific immune response to Y. pestis infection. J. Biol. Chem. 285: 10832–10840.

Brenner, T. J., and C. Guthrie, 2006   Assembly of Snu114 into U5 snRNP requires Prp8 and a functional GTPase domain. RNA 12: 862–871.

Burns, K., S. Janssens, B. Brissoni, N. Olivos, R. Beyaert et al., 2003   Inhibition of interleukin 1 receptor/Toll-like receptor signaling through the alternatively spliced, short form of MyD88 is due to its failure to recruit IRAK-4. J. Exp. Med. 197: 263–268.

Calzado, M. A., S. Bacher, and M. L. Schmitz, 2007   NF-kappaB inhibitors for the treatment of inflammatory diseases and cancer. Curr. Med. Chem. 14: 367–376.

Chang, J. T., and J. R. Nevins, 2006   GATHER: a systems approach to interpreting genomic signatures. Bioinformatics 22: 2926–2933.

Collins, L. J., C. G. Kurland, P. Biggs, and D. Penny, 2009   The modern RNP world of eukaryotes. J. Hered. 100: 597–604.

Conboy, I. M., D. Manoli, V. Mhaiskar, and P. P. Jones, 1999   Calcineurin and vacuolar-type H+-ATPase modulate macrophage effector functions. Proc. Natl. Acad. Sci. USA 96: 6324–6329.

Connolly, D. J., and L. A. O'Neill, 2012   New developments in Toll-like receptor targeted therapeutics. Curr. Opin. Pharmacol. 12: 510–518.

Cook, D. N., D. S. Pisetsky, and D. A. Schwartz, 2004   Toll-like receptors in the pathogenesis of human disease. Nat. Immunol. 5: 975–979.

Corrionero, A., B. Minana, and J. Valcarcel, 2011   Reduced fidelity of branch point recognition and alternative splicing induced by the anti-tumor drug spliceostatin A. Genes Dev. 25: 445–459.

Couillault, C., N. Pujol, J. Reboul, L. Sabatier, J. F. Guichou et al., 2004   TLR-independent control of innate immunity in Caenorhabditis elegans by the TIR domain adaptor protein TIR-1, an ortholog of human SARM. Nat. Immunol. 5: 488–494.

Coux, O., K. Tanaka, and A. L. Goldberg, 1996   Structure and functions of the 20S and 26S proteasomes. Annu. Rev. Biochem. 65: 801–847.

De Arras, L., and S. Alper, 2013   The Sf3a mRNA splicing complex mediates a MyD88-dependent negative feedback loop that limits the innate immune response. PLoS Genet. 9: e1003855.

De Arras, L., I. V. Yang, B. Lackford, D. W. Riches, R. Prekeris et al., 2012   Spatiotemporal Inhibition of Innate Immunity Signaling by the Tbc1d23 RAB-GAP. J. Immunol. 188: 2905–2913.

De Arras, L., A. Seng, B. Lackford, M. Keikhaee, B. Bowerman et al., 2013   An evolutionarily conserved innate immunity protein interaction network. J. Biol. Chem. 288: 1967–1978.

Dillin, A., D. K. Crawford, and C. Kenyon, 2002   Timing requirements for insulin/IGF-1 signaling in C. elegans. Science 298: 830–834.

Drory, O., F. Frolow, and N. Nelson, 2004   Crystal structure of yeast V-ATPase subunit C reveals its stator function. EMBO Rep. 5: 1148–1152.

Elliott, P. J., T. M. Zollner, and W. H. Boehncke, 2003   Proteasome inhibition: a new anti-inflammatory strategy. J. Mol. Med. 81: 235–245.

Engelmann, I., and N. Pujol, 2010   Innate immunity in C. elegans. Adv. Exp. Med. Biol. 708: 105–121.

Ewbank, J. J., 2006   Signaling in the immune response (January 23, 2006), WormBook, ed. The C. elegans Research Community, WormBook, doi/10.1895/wormbook.1.83.1, http://www.wormbook.org.

Ewbank, J. J., and O. Zugasti, 2011   C. elegans: model host and tool for antimicrobial drug discovery. Dis. Model. Mech. 4: 300–304.

Fabrizio, P., B. Laggerbauer, J. Lauber, W. S. Lane, and R. Luhrmann, 1997   An evolutionarily conserved U5 snRNP-specific protein is a GTP-binding factor closely related to the ribosomal translocase EF-2. EMBO J. 16: 4092–4106.

Fan, L., C. Lagisetti, C. C. Edwards, T. R. Webb, and P. M. Potter, 2011   Sudemycins, novel small molecule analogues of FR901464, induce alternative gene splicing. ACS Chem. Biol. 6: 582–589.

Fernandez-Botran, R., and V. Větvička, 2001   Methods in Cellular Immunology, CRC Press, Boca Raton.

Foley, E., and P. H. O'Farrell, 2004   Functional dissection of an innate immune response by a genome-wide RNAi screen. PLoS Biol. 2: E203.

Forgac, M., 1999 Structure and properties of the vacuolar (H+)-ATPases. J. Biol. Chem. 274: 12951–12954.

Garsin, D. A., C. D. Sifri, E. Mylonakis, X. Qin, K. V. Singh et al., 2001 A simple model host for identifying Gram-positive virulence factors. Proc. Natl. Acad. Sci. USA 98: 10892–10897.

Goh, F. G., and K. S. Midwood, 2012 Intrinsic danger: activation of Toll-like receptors in rheumatoid arthritis. Rheumatology (Oxford) 51: 7–23.

Gordon, C. T., F. Petit, M. Oufadem, C. Decaestecker, A. S. Jourdain et al., 2012 EFTUD2 haploinsufficiency leads to syndromic oesophageal atresia. J. Med. Genet. 49: 737–746.

Ho, M. N., K. J. Hill, M. A. Lindorfer, and T. H. Stevens, 1993 Isolation of vacuolar membrane H(+)-ATPase-deficient yeast mutants; the VMA5 and VMA4 genes are essential for assembly and activity of the vacuolar H(+)-ATPase. J. Biol. Chem. 268: 221–227.

Huffman, D. L., L. Abrami, R. Sasik, J. Corbeil, F. G. van der Goot et al., 2004 Mitogen-activated protein kinase pathways defend against bacterial pore-forming toxins. Proc. Natl. Acad. Sci. USA 101: 10995–11000.

Irazoqui, J., and F. Ausubel, 2010 99th Dahlem Conference on infection, inflammation, and chronic inflammatory disorders: Caenorhabditis elegans as a model to study tissues involved in host immunity and microbial pathogenesis. Clin. Exp. Immunol. 160: 48–57.

Iwasaki, A., and R. Medzhitov, 2010 Regulation of adaptive immunity by the innate immune system. Science 327: 291–295.

Janssens, S., K. Burns, J. Tschopp, and R. Beyaert, 2002 Regulation of interleukin-1- and lipopolysaccharide-induced NF-kappaB activation by alternative splicing of MyD88. Curr. Biol. 12: 467–471.

Janssens, S., K. Burns, E. Vercammen, J. Tschopp, and R. Beyaert, 2003 MyD88S, a splice variant of MyD88, differentially modulates NF-kappaB- and AP-1-dependent gene expression. FEBS Lett. 548: 103–107.

Kamath, R. S., and J. Ahringer, 2003 Genome-wide RNAi screening in Caenorhabditis elegans. Methods 30: 313–321.

Kamath, R. S., A. G. Fraser, Y. Dong, G. Poulin, R. Durbin et al., 2003 Systematic functional analysis of the Caenorhabditis elegans genome using RNAi. Nature 421: 231–237.

Karin, M., and F. R. Greten, 2005 NF-kappaB: linking inflammation and immunity to cancer development and progression. Nat. Rev. Immunol. 5: 749–759.

Kaufmann, S. H. E., R. Medzhitov, S. Gordon, 2004 The Innate Immune Response to Infection. ASM Press, Washington D.C.

Kawai, T., and S. Akira, 2010 The role of pattern-recognition receptors in innate immunity: update on Toll-like receptors. Nat. Immunol. 11: 373–384.

Kennedy, S., D. Wang, and G. Ruvkun, 2004 A conserved siRNA-degrading RNase negatively regulates RNA interference in C. elegans. Nature 427: 645–649.

Kim, D. H., R. Feinbaum, G. Alloing, F. E. Emerson, D. A. Garsin et al., 2002 A conserved p38 MAP kinase pathway in Caenorhabditis elegans innate immunity. Science 297: 623–626.

Kramer, A., 1996 The structure and function of proteins involved in mammalian pre-mRNA splicing. Annu. Rev. Biochem. 65: 367–409.

Kramer, A., F. Ferfoglia, C. J. Huang, F. Mulhaupt, D. Nesic et al., 2005 Structure-function analysis of the U2 snRNP-associated splicing factor SF3a. Biochem. Soc. Trans. 33: 439–442.

Lee, H. K., and A. Iwasaki, 2007 Innate control of adaptive immunity: dendritic cells and beyond. Semin. Immunol. 19: 48–55.

Liberati, N. T., K. A. Fitzgerald, D. H. Kim, R. Feinbaum, D. T. Golenbock et al., 2004 Requirement for a conserved Toll/interleukin-1 resistance domain protein in the Caenorhabditis elegans immune response. Proc. Natl. Acad. Sci. USA 101: 6593–6598.

Lines, M. A., L. Huang, J. Schwartzentruber, S. L. Douglas, D. C. Lynch et al., 2012 Haploinsufficiency of a spliceosomal GTPase encoded by EFTUD2 causes mandibulofacial dysostosis with microcephaly. Am. J. Hum. Genet. 90: 369–377.

Luquetti, D. V., A. V. Hing, M. J. Rieder, D. A. Nickerson, E. H. Turner et al., 2013 "Mandibulofacial dysostosis with microcephaly" caused by EFTUD2 mutations: expanding the phenotype. Am. J. Med. Genet. A. 161A: 108–113.

Mahajan-Miklos, S., M. W. Tan, L. G. Rahme, and F. M. Ausubel, 1999 Molecular mechanisms of bacterial virulence elucidated using a Pseudomonas aeruginosa-Caenorhabditis elegans pathogenesis model. Cell 96: 47–56.

Mallo, G. V., C. L. Kurz, C. Couillault, N. Pujol, S. Granjeaud et al., 2002 Inducible antibacterial defense system in C. elegans. Curr. Biol. 12: 1209–1214.

Martinon, F., X. Chen, A. H. Lee, and L. H. Glimcher, 2010 TLR activation of the transcription factor XBP1 regulates innate immune responses in macrophages. Nat. Immunol. 11: 411–418.

Meissner, B., A. Warner, K. Wong, N. Dube, A. Lorch et al., 2009 An integrated strategy to study muscle development and myofilament structure in Caenorhabditis elegans. PLoS Genet. 5: e1000537.

Mendoza-Barbera, E., M. A. Corral-Rodriguez, A. Soares-Schanoski, M. Velarde, S. Macieira et al., 2009 Contribution of globular death domains and unstructured linkers to MyD88.IRAK-4 heterodimer formation: an explanation for the antagonistic activity of MyD88s. Biochem. Biophys. Res. Commun. 380: 183–187.

Mi, H., Q. Dong, A. Muruganujan, P. Gaudet, S. Lewis et al., 2010 PANTHER version 7: improved phylogenetic trees, orthologs and collaboration with the Gene Ontology Consortium. Nucleic Acids Res. 38: D204–D210.

Mitchell, D. H., J. W. Stiles, J. Santelli, and D. R. Sanadi, 1979 Synchronous growth and aging of Caenorhabditis elegans in the presence of fluorodeoxyuridine. J. Gerontol. 34: 28–36.

Mochii, M., S. Yoshida, K. Morita, Y. Kohara, and N. Ueno, 1999 Identification of transforming growth factor-beta- regulated genes in Caenorhabditis elegans by differential hybridization of arrayed cDNAs. Proc. Natl. Acad. Sci. USA 96: 15020–15025.

Muhammed, M., B. B. Fuchs, M. P. Wu, J. Breger, J. J. Coleman et al., 2012 The role of mycelium production and a MAPK-mediated immune response in the C. elegans-Fusarium model system. Med. Mycol. 50: 488–496.

Mullick, A. E., P. S. Tobias, and L. K. Curtiss, 2005 Modulation of atherosclerosis in mice by Toll-like receptor 2. J. Clin. Invest. 115: 3149–3156.

Murphy, C. T., S. A. McCarroll, C. I. Bargmann, A. Fraser, R. S. Kamath et al., 2003 Genes that act downstream of DAF-16 to influence the lifespan of Caenorhabditis elegans. Nature 424: 277–283.

Newman, A. J., 1997 The role of U5 snRNP in pre-mRNA splicing. EMBO J. 16: 5797–5800.

Nishi, T., and M. Forgac, 2002 The vacuolar (H+)-ATPases–nature's most versatile proton pumps. Nat. Rev. Mol. Cell Biol. 3: 94–103.

O'Rourke, D., D. Baban, M. Demidova, R. Mott, and J. Hodgkin, 2006 Genomic clusters, putative pathogen recognition molecules, and antimicrobial genes are induced by infection of C. elegans with M. nematophilum. Genome Res. 16: 1005–1016.

Picard, C., J. L. Casanova, and A. Puel, 2011 Infectious diseases in patients with IRAK-4, MyD88, NEMO, or IkappaBalpha deficiency. Clin. Microbiol. Rev. 24: 490–497.

Powell, J. R., and F. M. Ausubel, 2008 Models of Caenorhabditis elegans infection by bacterial and fungal pathogens. Methods Mol. Biol. 415: 403–427.

Pujol, N., E. M. Link, L. X. Liu, C. L. Kurz, G. Alloing et al., 2001 A reverse genetic analysis of components of the Toll signaling pathway in Caenorhabditis elegans. Curr. Biol. 11: 809–821.

Pukkila-Worley, R., and F. M. Ausubel, 2012 Immune defense mechanisms in the Caenorhabditis elegans intestinal epithelium. Curr. Opin. Immunol. 24: 3–9.

Pulverer, B., 2003 Whither RNAi? Nat Cell Biol 5: 489–90.

Rahme, L. G., E. J. Stevens, S. F. Wolfort, J. Shao, R. G. Tompkins *et al.*, 1995 Common virulence factors for bacterial pathogenicity in plants and animals. Science 268: 1899–1902.

Richardson, C. E., T. Kooistra, and D. H. Kim, 2010 An essential role for XBP-1 in host protection against immune activation in C. elegans. Nature 463: 1092–1095.

Rino, J., and M. Carmo-Fonseca, 2009 The spliceosome: A self-organized macromolecular machine in the nucleus? Trends Cell Biol. 19: 375–384.

Sayers, E. W., T. Barrett, D. A. Benson, E. Bolton, S. H. Bryant *et al.*, 2012 Database resources of the National Center for Biotechnology Information. Nucleic Acids Res. 40: D13–D25.

Shapira, M., B. J. Hamlin, J. Rong, K. Chen, M. Ronen *et al.*, 2006 A conserved role for a GATA transcription factor in regulating epithelial innate immune responses. Proc. Natl. Acad. Sci. USA 103: 14086–14091.

Shen, J., J. Reis, D. C. Morrison, C. Papasian, S. Raghavakaimal *et al.*, 2006 Key inflammatory signaling pathways are regulated by the proteasome. Shock 25: 472–484.

Small, E. C., S. R. Leggett, A. A. Winans, and J. P. Staley, 2006 The EF-G-like GTPase Snu114p regulates spliceosome dynamics mediated by Brr2p, a DExD/H box ATPase. Mol. Cell 23: 389–399.

Smith, A. N., R. C. Lovering, M. Futai, J. Takeda, D. Brown *et al.*, 2003 Revised nomenclature for mammalian vacuolar-type H+-ATPase subunit genes. Mol. Cell 12: 801–803.

Sperling, J., M. Azubel, and R. Sperling, 2008 Structure and function of the Pre-mRNA splicing machine. Structure 16: 1605–1615.

Stevens, T. H., and M. Forgac, 1997 Structure, function and regulation of the vacuolar (H+)-ATPase. Annu. Rev. Cell Dev. Biol. 13: 779–808.

Takeuchi, O., and S. Akira, 2010 Pattern recognition receptors and inflammation. Cell 140: 805–820.

Tan, M. W., S. Mahajan-Miklos, and F. M. Ausubel, 1999 Killing of Caenorhabditis elegans by Pseudomonas aeruginosa used to model mammalian bacterial pathogenesis. Proc. Natl. Acad. Sci. USA 96: 715–720.

Tenor, J. L., and A. Aballay, 2007 A conserved Toll-like receptor is required for Caenorhabditis elegans innate immunity. EMBO Rep. 9: 103–109.

Troemel, E. R., S. W. Chu, V. Reinke, S. S. Lee, F. M. Ausubel *et al.*, 2006 p38 MAPK regulates expression of immune response genes and contributes to longevity in C. elegans. PLoS Genet. 2: e183.

Turner, I. A., C. M. Norman, M. J. Churcher, and A. J. Newman, 2004 Roles of the U5 snRNP in spliceosome dynamics and catalysis. Biochem. Soc. Trans. 32: 928–931.

Updike, D. L., and S. Strome, 2009 A genomewide RNAi screen for genes that affect the stability, distribution and function of P granules in Caenorhabditis elegans. Genetics 183: 1397–1419.

Visconte, V., H. J. Rogers, J. Singh, J. Barnard, M. Bupathi *et al.*, 2012 SF3B1 haploinsufficiency leads to formation of ring sideroblasts in myelodysplastic syndromes. Blood 120: 3173–3186.

Voigt, C., A. Megarbane, K. Neveling, J. C. Czeschik, B. Albrecht *et al.*, 2013 Oto-facial syndrome and esophageal atresia, intellectual disability and zygomatic anomalies: expanding the phenotypes associated with EFTUD2 mutations. Orphanet J. Rare Dis. 8: 110.

Wahl, M. C., C. L. Will, and R. Luhrmann, 2009 The spliceosome: design principles of a dynamic RNP machine. Cell 136: 701–718.

Wang, J., and M. A. Maldonado, 2006 The ubiquitin-proteasome system and its role in inflammatory and autoimmune diseases. Cell. Mol. Immunol. 3: 255–261.

Wood, W. B., 1988 *The Nematode Caenorhabditis elegans*, Cold Spring Harbor Laboratory Press, Cold Spring Harbor, NY.

Yook, K., T. W. Harris, T. Bieri, A. Cabunoc, J. Chan *et al.*, 2012 WormBase 2012: more genomes, more data, new website. Nucleic Acids Res. 40: D735–D741.
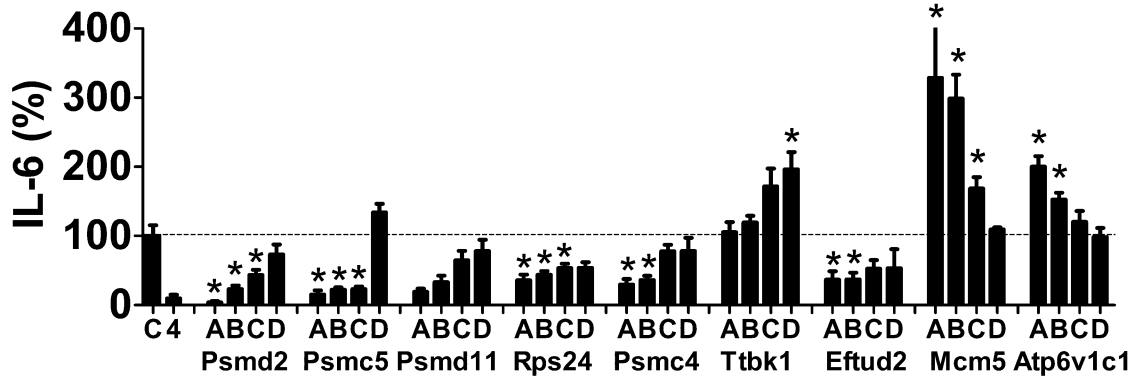
Communicating editor: B. Lazzaro

GENETICS

# Comparative Genomics RNAi Screen Identifies Eftud2 as a Novel Regulator of Innate Immunity

Lesly De Arras, Rebecca Laws, Sonia M. Leach, Kyle Pontis, Jonathan H. Freedman,
David A. Schwartz, and Scott Alper

Figure S1   Use of individual siRNA duplexes to confirm the effect of candidate innate immunity regulators. Four individual siRNA duplexes (labeled A through D) for the indicated genes were transfected into the RAW264.7 cell line, cells were stimulated with 20 ng/ml LPS for six hours, and IL-6 production was monitored by ELISA. C refers to non-targeting control siRNA, 4 refers to positive control TLR4 siRNA.

L. De Arras *et al.*
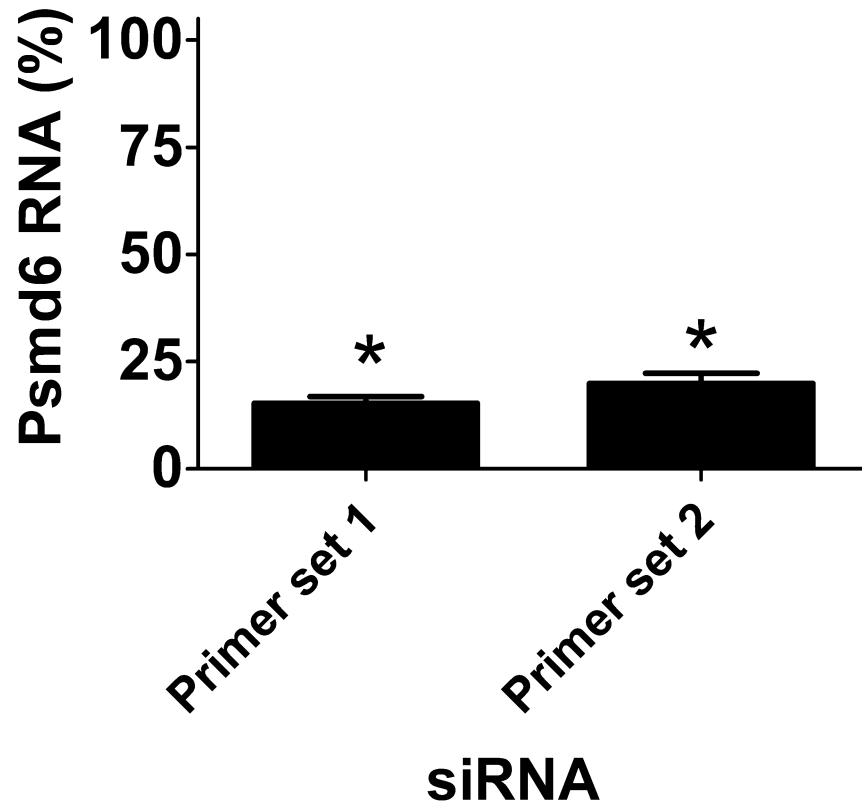
Figure S2 siRNA-mediated gene knockdown of Psmd6 was monitored by qPCR using either of two different primer sets.
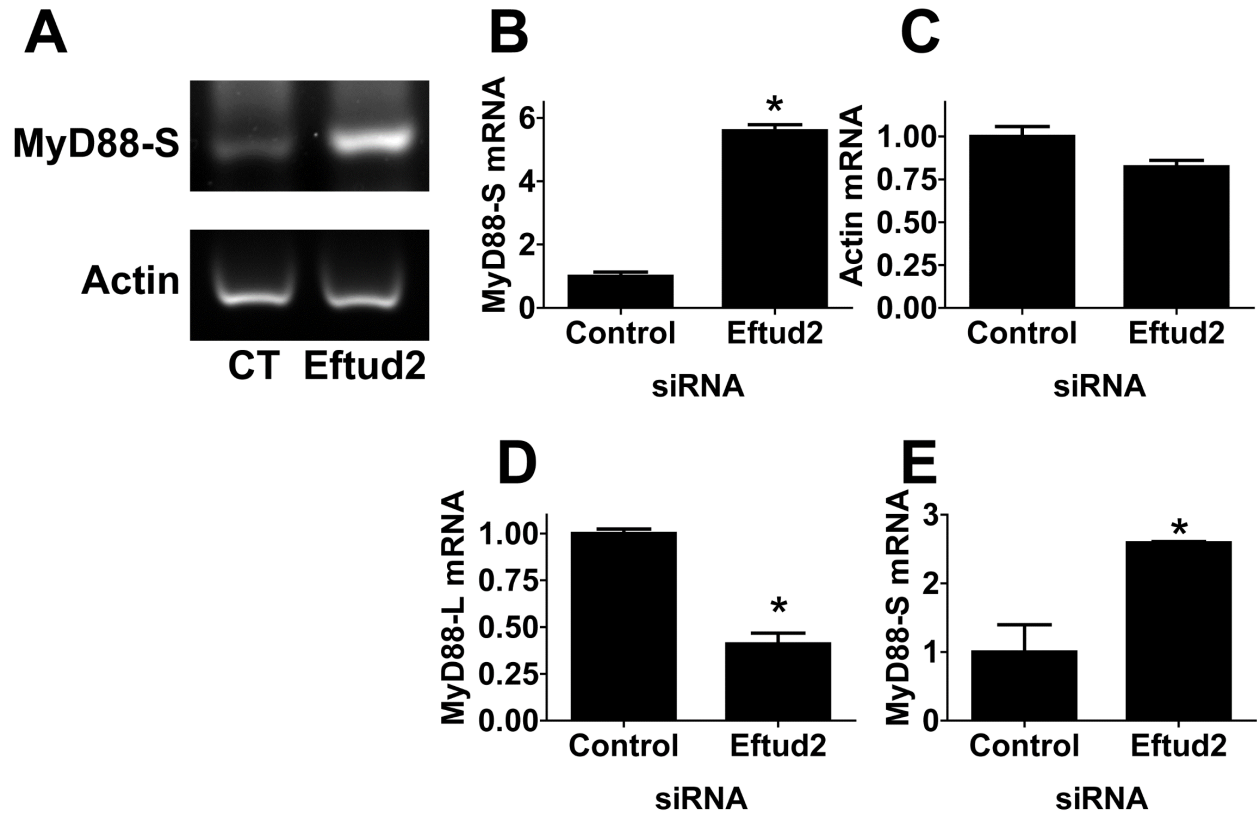
Figure S3 RT-PCR demonstrates that Eftud2 regulates the alternative mRNA splicing of MyD88. Cells were exposed to either Eftud2 siRNA or control non-targetting siRNA (CT), were then treated with 20 ng/ml LPS for six hours, RNA was extracted, RT-PCR was performed to amplify the indicated mRNAs, and the amplified products were analyzed by agarose gel electrophoresis. (A) Representative images of PCR products specific for either MyD88$_S$ or βactin. (B,C) Quantitation of MyD88$_S$ and βactin from three independent experiments. (E,F) RT-PCR using primers that bracket MyD88 exon 2 was performed to simultaneously amplify both MyD88$_L$ and MyD88$_S$ (Figure 6G). Depicted is quantitation of MyD88$_L$ and MyD88$_S$ from three independent experiments.

Table S1   Complete *C. elegans* RNAi retest data. Compilation of all data from each individual well for all retests and original genomic screen (indicated by *). GFP % calculated compared to control RNAi wells on retest plates and compared to average of whole plate for genomic screen. ** indicates gene that differs from library annotation based on our sequencing. Data from TOF bin 150-350. Wells with n<5 in the retests for this bin are not displayed.

Available for download as an Excel file at http://www.genetics.org/lookup/suppl/doi:10.1534/genetics.113.160499/-/DC1

Table S2 Oligonucleotides used for qPCR and RT-PCR

Gene	Left primer	Right primer
βactin	CTGAACCCTAAGGCCAACCGTG	CCGTCTCCGGAGTCCATCACAATG
IL-6	CTTGGGACTGATGCTGGTGAC	GCCTCCGACTTGTGAAGTGGTATAGACAGG
Psmd2	GCT ACC TGT AAT GGG AGA TTC CAA GTC CAG C	GAT GGT CTG AAG GAT GGT GGA AGT GAC ATC TCC
Psmc5	CTG TCC AAG ATT GAA GAA CTC CAG TTG ATT G	CAG CTG CAG CTC CTC CCG CAA CAG GCG AAC TTT TG
Psmd11	GGC TCA AGC TAG CAA GAA CAG ATC ACT GGC AG	CGG ATC AGA TTC TGT TCC AGT AAG TTA TCG TAC AG
Rps24	CCT CTT TTC CTC CTC TCC AGC TCC GGC GCC GTA G	CTC TGA AGC AGA CGG TTG GTC ATG AAC TTC CTG G
Psmc4	CGA CAG CAG CAT CAT GAT GCT CAC CTC AGA CCA G	CAC CTC CTG CTT CTG GAT GTC CAT GCC TCC G
Ttbk1	CTG GAC CAC ATT GCC AGC CTC GAC TAC TTC ACC	CTC CCA GTC AAA GGC CTC GTT CTC GGC AAT GCC
Eftud2	CAT AGT CCA GGA GGA AGA CAC CCA GCC CCT CAC AG	CTC AGA GTT GTC CAT CAG ATC TGC TAA GAA ATC CA
Mcm5	TGC TCA AGT CAG ATG CCA GCC CGT CGA GCA TTC GG	GCT GAA ATG ATG ATG CCA GGG ATC TTC ACC AGG TG
Atp6v1c1	CGG ATG AAC TGG CTA AAC TGG ATG CAT TTG TAG	GCT GTC CTC CAG CAC ATC AGC CAT GTA CTG AG
Psmd6 #1	CAG TAT GAT CGC CTT AGA AAG GCC GGA CCT CAG G	AAC AGA TAC TGC CGA ACT GCT GGA AGA CTG TG
Psmd6 #2	GGT GTG GGT GTG GAC TTC ATT GAC CAG GAG CTG	GCC AGT TCT TGC TAT CAG GTC TGT TGG TCT CCA CG
MyD88-S	GGAGCTGAAGTCGCGCATCGGACAAAC	GTCTGTTCTAGTTGCCGGATCATCTCCTGCAC
MyD88-L	GTCTGTTCTAGTTGCCGGATCATCTCCTGCAC	CCACCCTTGATGACCCCTAGGACAAAC
MyD88-S PCR	TTGTTGGATGCCTGGCAGGGGCGCTCTGGC	GTTCCGGCGTTTGTCCGATGC
MyD88-L/S PCR	CTGTCGGCAGGCTGCTAGAGCTGCTGGCC	CATCTCCTGCACAAACTCGATATCGTTGGGGC
oligo-dT	from Promega	
MyD88 RT	GCTGTCCCAAAGGAAACACACATATGCAGATGCC	

Table S3   Pathways that affect *clec-85* expression in *C. elegans*

#	Annotation	p value
1	GO:0019941 [9]: modification-dependent protein catabolism	0.005
2	GO:0006511 [10]: ubiquitin-dependent protein catabolism	0.005
3	GO:0044257 [7]: cellular protein catabolism	0.009
4	GO:0006508 [8]: proteolysis and peptidolysis	0.009
5	GO:0030163 [6]: protein catabolism	0.010
6	GO:0043285 [5]: biopolymer catabolism	0.010
7	GO:0044265 [6]: cellular macromolecule catabolism	0.011
8	GO:0009057 [5]: macromolecule catabolism	0.011
9	GO:0044248 [5]: cellular catabolism	0.012
10	GO:0009056 [4]: catabolism	0.012
11	GO:0019538 [5]: protein metabolism	0.013
12	GO:0044267 [6]: cellular protein metabolism	0.013
13	GO:0044260 [5]: cellular macromolecule metabolism	0.014
14	GO:0043283 [4]: biopolymer metabolism	0.014
15	GO:0043170 [4]: macromolecule metabolism	0.015
16	GO:0044238 [4]: primary metabolism	0.034
17	GO:0044237 [4]: cellular metabolism	0.038
18	GO:0008152 [3]: metabolism	0.044

Table S4 Survival data from Fig. 4

Panel A	RNAi	Median survival (hrs)	n	*P* value
P. aeruginosa				
	Control	74	134	
	eftu-2	48.5	106	<0.0001
	vha-11	15	131	<0.0001

Panel B	RNAi	Median survival (days)	n	*P* value
E. coli				
	Control	12	88	
	eftu-2	13	83	0.0001
	vha-11	4	91	<0.0001

Panel C	RNAi	Median survival (days)	n	*P* value
Live *E. coli*	Control	14	124	
Live *E. coli*	*vha-11*	6	126	< 0.0001
Heat killed *E. coli*	Control	15	92	< 0.0001
Heat killed *E. coli*	*vha-11*	6	95	< 0.0001

L. De Arras *et al.*